Optomechanical Imaging: Biomechanic and Hemodynamic Responses of the Breast to Controlled Articulation

Rabah Al abdi[1], Gavriel Feuer[1], Harry L. Graber[1,2], Subrata Saha[1], and Randall L. Barbour[1,2]
[1]SUNY Downstate Medical Center,450 Clarkson Ave, Brooklyn NY 11203
[2]NIRx Medical Technologies LLC., 15 Cherry Lane, Glen Head NY 11545
(718)-270-1286, (718)-613-8774 (Fax), rabah.alabdi@downstate.edu

Abstract: The optomechanical response of the breast was explored during fine articulation as a function of the applied force protocol. Comparisons between calculated internal pressure or stress maps and reconstructed hemodynamic images show strong correlations.
OCIS codes: (120.5475) Pressure measurement; (170.2655) Functional monitoring and imaging.

1. Introduction

There are many instances where the details of blood delivery to tissue and bulk fluid redistribution among the various tissue compartments can be impacted by disease or trauma. For instance, a common phenotype of breast cancer is derangements in hemodynamic states accompanied by increased tissue stiffness and local edema [1]. Motivated by the hypothesis that externally applied mechanical forces can produce distinct dynamic responses among these various compartments, we have recently developed working technology as a new approach for assessment of pathology of the breast and other soft tissues. Principal elements of this technology, referred to as optomechanical imaging [2], include concurrent bilateral measures of the viscoelastic and hemodynamic properties of the breast in response to a wide range of controlled articulation maneuvers. Encouraging evidence was reported of high-contrast tumor detection in response to these maneuvers [2].

To better appreciate the expected influence that externally applied forces have on internal fluid shifts, here we have compared the measured hemodynamic response of the breast to modeled estimates of internal mechanical forces as a function of various applied articulation maneuvers. Taking the lead from Darling *et al.* [3], we have estimated the internal thermodynamic pressure p (alternatively referred to as the interstitial fluid pressure), and other related metrics, of the breast in response to specified maneuvers. Results obtained strongly suggest that mechanical modeling is a useful approach to predicting bulk hemodyamic responses to controlled articulations.

2. Methods

2.1. Experiment. Simultaneous bilateral breast imaging was performed using a newly developed optomechnical imaging system described by Al abdi *et al.* ("Breast Cancer Detection by Optomechanical Imaging," this conference). The described system provides for high optode-density CW-NIRS DOT imaging, accommodates a wide range of breast sizes, and simultaneously measures the viscoelastic response of the breast to finely controlled articulations.

Figure 1 shows a schematic of the sensing heads used for data collection and articulation, together with the FEM model used for mechanical forward-problem computations and for solving the optical inverse problem. Full-compression protocols involved applying 28 kPa of pressure to every articulating element (AE); partial compression involved applying similar forces, either to the medial and lateral AEs only, or to the craniocaudal AEs only.

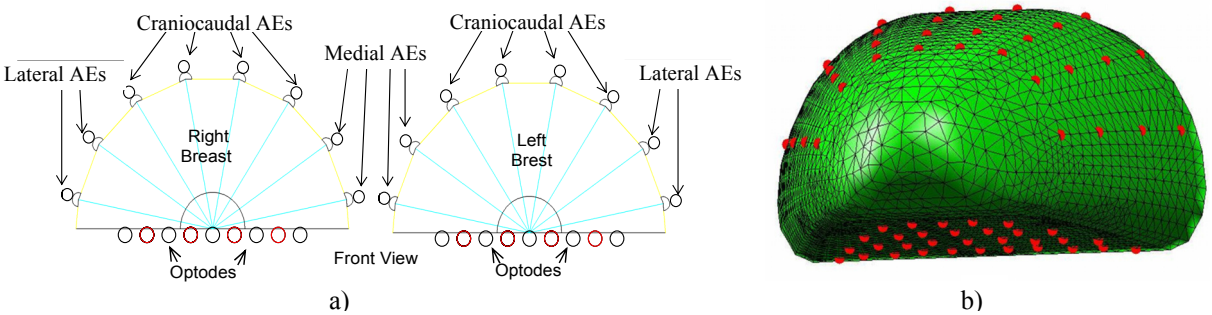

Fig. 1: (a) A schematic of the location of the support rods relative to the left and right breasts, (b) finite element mesh used for inverse hemodynamic computations. A similar shape was used for the forward mechanical model computations.

2.2. Modeling. The mechanical properties of soft tissue typically are nonlinear and viscoelastic. However, if the strains are restricted to sufficiently small ranges, soft-tissue mechanical responses can be well approximated with linear elasticity theory [4]. For calculations of p, breast tissue can be modeled as a solid material containing fluid cavities, which can be approximated at a macroscopic level as a poroelastic substrate [5]. Fluid migration in a poroelastic material having a linear elastic solid component can be described by the following equations for conservation of mass and of momentum, respectively:

$$\nabla \cdot \dot{u} - \nabla \cdot \left(\kappa \nabla p \right) + \chi p = 0, \tag{1}$$

$$\nabla \cdot \boldsymbol{\sigma} = \nabla \cdot \left(-p\mathbf{I} + \lambda \nabla \cdot u\mathbf{I} + 2\mu\boldsymbol{\varepsilon} \right) = 0, \tag{2}$$

where u and $\dot{u}$ are the displacement and velocity of the solid phase, respectively; $\mathbf{I}$ is the identity matrix; $\boldsymbol{\sigma}$ and $\boldsymbol{\varepsilon}$ are the stress and strain tensors, respectively; and κ (interstitial permeability) and χ (average microfiltration rate) are tissue constitutive properties that govern the motion of the fluid component in response to applied force. We introduce the simplifying assumptions that surface tensions and the effects of body forces (e.g., gravity) are negligible, and that $\kappa \approx 0$ and $\chi \approx 0$ under the applied conditions (i.e., evaluation of mechanical properties during a brief time interval that immediately follows a rapid compression). The time course of the modeled protocol additionally gives us $\dot{u} \approx 0$ (i.e., there is negligible creep). Therefore, Eq. (1) can be safely neglected. (If non-zero κ, χ or $\dot{u}$ were modeled, the practical impact would be to dampen and spatially smear out the internal responses to applied force.)

The microscopic analogue of Eq. (2), which is the basis of the forward-modeling computations, is:

$$\tau_{ij} = -p\delta_{ij} + \lambda tr\left(\boldsymbol{\varepsilon}\right)\delta_{ij} + \mu\left(\frac{\partial v_i}{\partial x_j} + \frac{\partial v_j}{\partial x_i} \right), \tag{3}$$

where τ_{ij} is the ij^{th} element of the surface stress tensor $\boldsymbol{\tau}$, δ_{ij} is the Kronecker delta, λ and μ are the Lamé parameters, $tr(\boldsymbol{\varepsilon})$ is the trace of the fluid strain tensor, and v is the fluid velocity. For a steady-state analysis, the velocity gradients in Eq. (3) can be equated with components of the strain [3]. By taking the mean of the axial components (i.e., $i = j$) of the stress, the thermodynamic pressure can be related to the mechanical pressure $\tilde{p}$ [which is defined as $\tilde{p} = -tr(\boldsymbol{\tau})/3$] and the principal strains as follows [3]:

$$p = \tilde{p} + \left(\lambda + \frac{2}{3}\mu \right) tr\left(\boldsymbol{\varepsilon}\right), \tag{4}$$

To calculate p, FEA was performed on a homogeneous model of breast tissue that has the mechanical properties appropriate for adipose tissue (i.e., Young's modulus = 19 kPa, Poisson's ratio = 0.495 [3]). The geometric model considered, shown in Fig. 1b, contains 3908 nodes and 16,761 finite elements and represents an approximation to the geometry of a typical breast when placed inside the breast imager's sensing head. Mechanical pressure, principal stresses, and principal strains were computed using nonlinear finite element software called FeBio (University of Utah, Salt Lake City), followed by calculation of the thermodynamic pressure by Eq. (4), and the effective stress by:

$$\sigma_v = \sqrt{\left[\left(\sigma_1 - \sigma_2\right)^2 + \left(\sigma_2 - \sigma_3\right)^2 + \left(\sigma_3 - \sigma_1\right)^2 \right] / 2}, \tag{5}$$

where the σ_is are the three principal stresses [6].

3. Results

Examples of model-computation and experimental results for three steady-state pressure protocols—compression by 1) all AEs sketched in Fig. 1a, 2) only the medial and lateral AEs, 3) only the craniocaudal AEs—are shown in Figure 2. Axial views of the calculated p and σ_v, following normalization of each image to its maximum value, are shown in Fig. 2a and 2b, respectively. Corresponding changes in the total hemoglobin responses (ΔHbT) derived from measurements taken on a healthy subject, are shown in Fig. 2c. Inspection reveals that, grossly, p is largest at the breast surfaces and decreases rapidly toward the center. On the other hand, σ_v tends to increase in moving from the surface to the center. At a more detailed level of inspection, the locations of the regions of maximal σ_v and p reflect, in an intuitively predictable way, the particular sets of AEs used for the compression and, in the case of p, additionally the lower boundary that corresponds to the measuring head's fixed bottom plate [2].

Inspection of the recovered ΔHbT spatial maps (Fig. 2c) indicates that they have strong spatial correlations with both p and σ_v (which also are noticeably correlated with each other). The inverse relationship between ΔHbT and σ_v (e.g., largest drops in ΔHbT occurring at or near the positions where σ_v is largest) is particularly striking. The

concurrence, between mechanical-properties computations for an idealized homogeneous medium and optical-properties reconstructions from experimental human-subject data, suggests that the observed hemodynamic-variable patterns represent redistributions of blood in response to changes in the internal stress distribution.

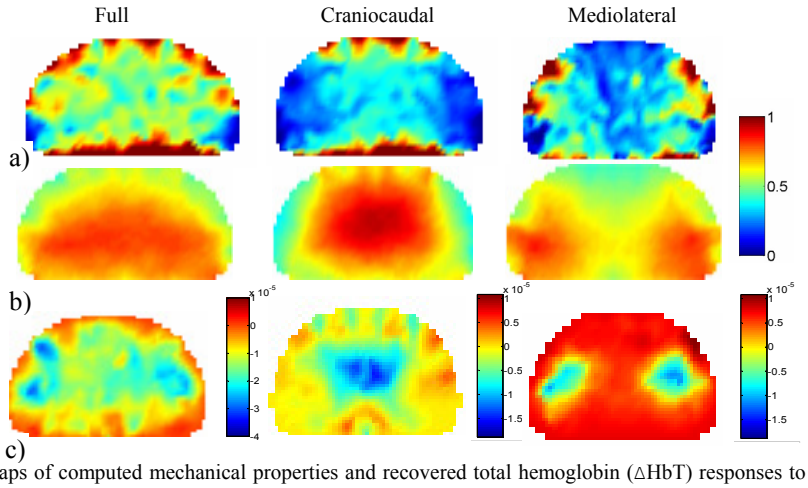

Fig. 2. Spatial maps of computed mechanical properties and recovered total hemoglobin (ΔHbT) responses to applied pressure. (a) Calculated thermodynamic pressure, (b) calculated effective stress, for a homogeneous poroelastic tissue model. (c) Reconstructed ΔHbT for a healthy research participant (57 years healthy women with D breast size and BMI of 27). Computations and measurements considered the same three compression protocols (28 kPa pressure in every case).

4. Summary

Applying pressure to the breast surface creates a complex heterogeneous pressure distribution within the tissue, and the spatial distribution of these forces is a function of the applied articulation maneuver and the tissue's material mechanical properties. The observation that there is a strong correlation between the measured hemodynamic response and computed spatial distributions of mechanical forces suggests that the simple poroelastic model considered can serve as a useful guide to predicting expected hemodynamic responses. By extension, we argue that deviations between the expected and measured responses would suggest the presence of phenomenologies (e.g., increased stiffness, enhanced angiogenesis) that affect underlying deterministic mechanisms linking the biomechanics and hemodynamics. While this relationship is undoubtedly complex, we are nevertheless hopeful that useful metrics that build on it can be derived. In the limit, and to a first approximation, one can certainly consider a cost function wherein the hemodynamic response is taken as inversely proportional to the effective stress, thereby supporting modeling of recursive solution schemes that update the distributions of both mechanical and hemodynamic properties. Also, as recognized in [2], factors affecting the vascular response can be independently manipulated in other ways in addition to applied-force maneuvers, such as by adjusting the composition of the inspired gases ("Carbogen Inspiration Enhances Hemodynamic Contrast in the Cancerous Breast," this conference), thereby leading to a wide range of differential responses that serve to discriminate healthy from cancerous breasts.

References

[1] P. Vaupel, "Blood perfusion and microenvironment of human tumors, implications for clinical radiooncology," in *Tumor Blood Flow*, M. Molls and P. Vaupel, eds. (Springer, 2000), 41-45.

[2] R. Al abdi, H.L. Graber, Y. Xu, and R.L. Barbour, "Optomechanical imaging system for breast cancer detection," *J. Optical Society of America A* **28**, 2473-2493 (2011).

[3] A. L. Darling, P. K. Yalavarthy, M. M. Doyley, H. Dehghani, and B. W. Pogue, "Interstitial fluid pressure in soft tissue as a result of an externally applied contact pressure," *Phys. Med. Biol.* **52**, 4121-4136 (2007).

[4] F. S. Azar, D. N. Metaxas, and M. D. Schnall, "A deformable finite element model of the breast for predicting mechanical deformations under external perturbations," *Acad. Radiol*. **8**, 965-975 (2001).

[5] R. Leiderman, P. E. Barbone, A. A. Oberai, and J. C. Bamber, "Coupling between elastic strain and interstitial flow: ramifications for poroelastic imaging," *Phys. Med. Biol.* **51**, 6291-6313 (2006).

[6] L. A. Pruitt and A. M. Chakravartula, *Mechanics of Biomaterials: Fundamental Principles for Implant Design* (Cambridge U. Press, 2011), pp. 245-251.

This research was supported by the National Institutes of Health (NIH) grant R41CA096102, U.S. Army grant DAMD017-03-C-0018, the Susan G. Komen Foundation, the New York State Department of Health (Empire Clinical Research Investigator Program), the New York State Foundation for Science, Technology and Innovation–Technology Transfer Incentive Program (NYSTAR-TIPP) grant C020041, and NIRx Medical Technologies.